GA–A27143

MODEL-BASED DECOUPLING CONTROL OF TOKAMAK PLASMAS

by
M.L. WALKER

OCTOBER 2011

GENERAL ATOMICS

DISCLAIMER

GA–A27143

MODEL-BASED DECOUPLING CONTROL OF TOKAMAK PLASMAS

by
M.L. WALKER

This is a preprint of a paper to be presented at the 2010 American Control Conference, September 23, 2011, in Montreal, Canada and to be published in Proceedings.

General Atomics, P.O. Box 85608, San Diego, California, USA

Work supported in part by
the U.S. Department of Energy
under DE-FC02-04ER54698

GENERAL ATOMICS PROJECT 30200
OCTOBER 2011

GENERAL ATOMICS

Model-Based Decoupling Control of Tokamak Plasmas

M. L. Walker, *Member, IEEE*

***Abstract*— Several model-based decoupling controllers have been simulated or implemented for control of plasmas in operating tokamaks. This type of control provides an appealing solution for those responsible for operating tokamaks because of the intuitive relationship between changes in control actuators and the response of controlled plasma parameters. We describe some of the decoupling control methods currently in use and under development for operating tokamaks as well as several practical issues associated with this choice of controller.**

I. INTRODUCTION

Tokamaks are torus (doughnut)-shaped devices designed to confine a plasma composed of ionized hydrogen isotopes while the plasma is heated to initiate fusion reactions. An illustration of a tokamak is provided in Fig. 1, which shows a cross section of the planned ITER [1] tokamak and plasma. Toroidal field coils (not shown), which produce a magnetic field oriented "into the page" in Figure 1, provide the largest (toroidal) magnetic field component in the tokamak, important for both force balance and stability. Magnetic fields produced by toroidal currents (currents flowing "into the page") in poloidal field (PF) coils are used to control the location of the plasma boundary, stabilize an open loop positional instability (the *vertical instability*) [2], and control the total toroidal current flowing in the plasma. In some tokamaks, a separate coil or coils may be assigned to a single one of these tasks. In others, a coil may simultaneously participate in more than one control task.

In this paper, we discuss some of the practical constraints that have led to an emphasis on decoupling control approaches in operating tokamaks. In Section II we describe the basic system model from which the various methods for decoupling can be derived. In Section III we first discuss the motivation for decoupling control in present devices, review approaches taken for decoupling the control of plasma boundary, current, and stability and analyze examples of application to new superconducting tokamaks. Finally, in Section IV we describe some limitations of the decoupling approach that must be considered when evaluating its potential application in the ITER device.

II. PLANT MODEL

The dynamics of the plasma current, vertical instability, and plasma shape are all described by the state equations [4]:

$$M_{cc}^{*}\dot{I}_c + R_c I_c + M_{cv}^{*}\dot{I}_v + M_{cp}^{*}\dot{I}_p = V_c \qquad (1a)$$

$$M_{vv}^{*}\dot{I}_v + R_v I_v + M_{vc}^{*}\dot{I}_c + M_{vp}^{*}\dot{I}_p = 0 \qquad (1b)$$

$$L_p^{*}\dot{I}_p + R_p I_p + M_{pc}^{*}\dot{I}_c + M_{pv}^{*}\dot{I}_v = V_{n.o.} \qquad (1c)$$

where I_c, I_v, and I_p represent toroidal currents in PF coils, vacuum vessel conductors (shown alternately shaded in Figure 1), and the plasma, respectively. V_c is the vector of voltages applied to the PF coils. Plasma current can be driven either by induction, where PF coil currents are ramped to produce nonzero current derivatives thereby inducing current in the plasma or by noninductive (*non-ohmic*) sources (see Tutorial 9 in [5]), represented by an effective voltage $V_{n.o.}$.

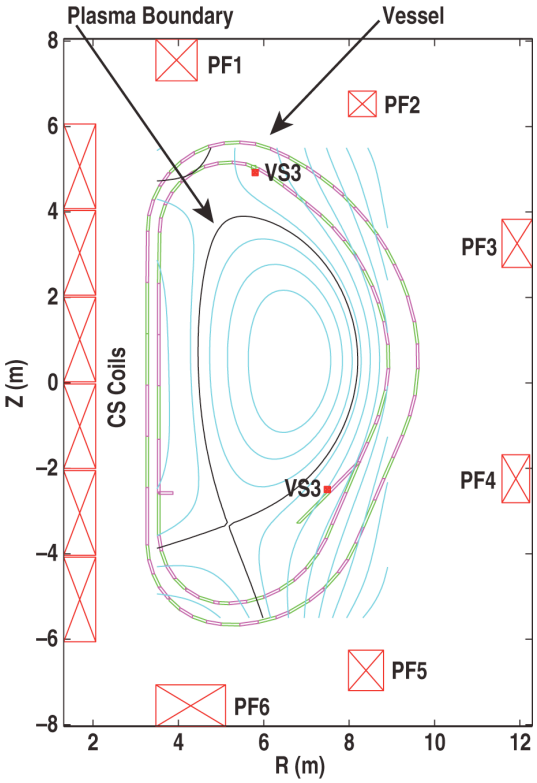

Figure 1. Cross-section of the ITER tokamak and plasma illustrating coils (PF and CS) used for control of the plasma boundary, position, and total current. Contours of constant magnetic flux are shown in blue, with the plasma boundary (black) defined as the outermost flux contour that closes upon itself. (See [3] for a definition of magnetic flux at a point, which leads to the concept of contours of constant flux.)

Manuscript received September 23, 2011. This work was supported in part by the US Department of Energy under DE-FC02-04ER54698 and DE-FG02-99ER54522.

M. L. Walker is with General Atomics, San Diego, CA (858-455-2483; fax: 858-455-4156; e-mail: walker@fusion.gat.com).

Matrices M^*_{ab} (with $L^*_p = M^*_{pp}$) are mutual inductance matrices for $a,b \in \{c,v,p\}$, which include the usual conductor-to-conductor mutual inductance as well as a plasma motion-induced inductance, linearized around the plasma equilibrium. The term plasma equilibrium refers to a balancing of competing forces rather than an equilibrium of the differential equation. The non-ohmic voltage is not an actual voltage, since the mechanisms (such as neutral beam or radio-frequency current drive) used to drive current directly do not impose an electric field. This is simply an artifice that is used to incorporate these sources of current drive into the circuit model paradigm by ascribing to them an equivalent voltage.

The mapping from currents to most outputs (in particular, the outputs in this paper) is expressed explicitly in terms of changes in current δI_* from equilibrium values [4]:

$$\delta y = C_{I_s}\delta I_s + C_{I_p}\delta I_p \quad , \tag{2}$$

where $\delta I_s = I_s - I_{s,eq}$, $\delta I_p = I_p - I_{p,eq}$, $\delta y = y - y_{eq}$, $I_s = \left[I_c^T, I_v^T\right]^T$, and the additional subscript "eq" denotes values at the plasma equilibrium from which the model equations (1) and (2) are derived. The output matrices C_{I_s} and C_{I_p} are computed as

$$\begin{aligned} C_{I_s} &= \frac{\partial y}{\partial I_s} + \frac{\partial y}{\partial r_C}\frac{\partial r_C}{\partial I_s} + \frac{\partial y}{\partial z_C}\frac{\partial z_C}{\partial I_s} \\ C_{I_p} &= \frac{\partial y}{\partial I_p} + \frac{\partial y}{\partial r_C}\frac{\partial r_C}{\partial I_p} + \frac{\partial y}{\partial z_C}\frac{\partial z_C}{\partial I_p} \end{aligned} \quad . \tag{3}$$

where r_C and z_C are radial and vertical position of the plasma current centroid ("center of mass" of the spatially distributed plasma current). The first term on the right in each expression represents the direct coupling from current sources to sensor measurements and the latter two terms in each represent the change in sensor measurement due to motion of the plasma caused by a change in current in the current sources. Including the two plasma terms creates output matrices C that include the *plasma response*. Removing those terms creates the *vacuum response*.

III. DECOUPLING CONTROL

Plasma poloidal field controllers on existing devices are dominated by a mixture of ad hoc and empirically tuned controllers. However, a gradually increasing number of model-based controllers are being tested and a few fielded for routine device operation. There are some constraints on this development however that tend to favor decoupling control solutions.

A. Motivations for Model-based Decoupling Control

On the next-generation ITER tokamak, currently under construction in southern France, it is accepted that model-based controllers will be required. The need for such controllers is driven by demanding performance requirements, limited experimental time for tuning, and reduced actuator margins relative to existing devices. The methods for model-based plasma controller development and validation by simulation must first be demonstrated to provide effective control on existing tokamaks. These demonstrations must include routine use of model-based controllers in daily operation. However, most of today's tokamaks operate very differently from the planned ITER operation. In ITER, a very limited number of plasma operating points will be targeted for control and therefore a greater effort may be focused on preparing control for those operating points. In contrast, most operating tokamaks frequently vary the plasmas produced and the conditions under which they must be controlled. Thus, routine use of a model-based shape/Ip/stabilization controllers in operation implies that those controllers must be effective over a broad range of plasmas and conditions, with some method of adaptation for new conditions required that is relatively fast (a few minutes to a few hours) and does not require a substantial knowledge of control theory.

These operational needs have led to a preference by experimental programs for simplicity and flexibility over optimality of control performance, which in turn has led to an emphasis on decoupling control. Even before mathematical models were available to support design of plasma controllers, some portions of machine design were tailored to provide decoupling of control parameters and thereby simplify operational control. One example of this is the use of one or more PF coils, known as ohmic coils, dedicated to control of only plasma current. Ohmic coils are designed to minimize the response of the plasma shape and position to changes in their current [6]. Similarly, separate coils for vertical control that have lower self-inductance and are closer to the plasma are sometimes incorporated into machine designs (e.g., VS3 in Fig. 1) to enable faster, more effective response to the instability. As will be seen in Section III-D, this enables a type of decoupling of vertical control from shape and plasma current control. In machines where hardware decoupling is not available, software methods of decoupling are often applied. Several of these methods are described in the following sections.

B. Decoupling of individual shape control parameters

The decoupling control approach typically attempted for plasma shape control is a form of static decoupling [7]. An early discussion of this approach in [8] approximates the steady-state boundary error response using a model of the vacuum response of magnetic flux and field at discrete locations on the plasma boundary to changes in coil current. More recent work incorporates the plasma response in the decoupling calculation [9].

The method for computing control errors proposed in [8] is often referred to as the *isoflux* method. This method exploits the capability of real time plasma equilibrium reconstruction algorithms to calculate the magnetic flux at all points within the tokamak vacuum vessel. Fig. 2 illustrates a plasma which was controlled in the DIII-D tokamak [6] using isoflux control and indicates quantities relevant to the control scheme. The real time reconstruction calculates the value of the poloidal flux in the vicinity of the plasma boundary. The controlled parameters are the values

of flux at prespecified control points along with the X–point R and Z positions. By requiring that the flux at each control point be equal to the same constant value, the control forces the same flux contour to pass through all of these control points. By choosing this constant value equal to the flux at the X–point, this flux contour must be the outermost closed flux surface, also known as the separatrix. The desired separatrix location is specified through a set of boundary control points (red diamonds) chosen from many such points on control segments. An X–point control grid is used to assist in calculating the X–point location by providing detailed flux and field information at a number of closely spaced points in the vicinity of the X–point. We will use this definition of control errors for examples in the following, but this particular choice of control error is not essential to the issues of decoupling discussed here.

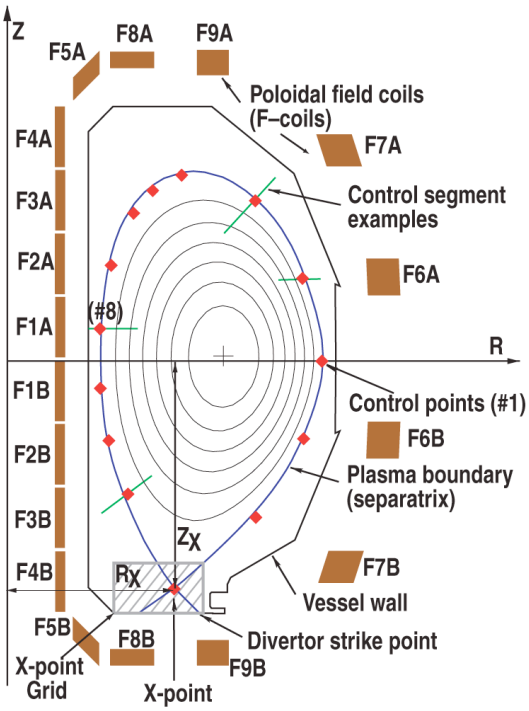

Figure 2. Isoflux control points and X point grid used for calculation of shape error. An X-point, denoted by R_X and Z_X represents a location where the boundary flux contour forms an X. It is also known as a null because the magnetic field becoming zero creates this effect. The ohmic coil dedicated to plasma current control is not shown.

The decoupling controller is developed by considering a matrix equation

$$GI_c = b \tag{4}$$

where G (computed from (3)) is the steady-state gain from coil currents I_c to boundary control errors b where

$$b = \left[\psi_1 - \psi_{ref} \quad \psi_2 - \psi_{ref} \quad \cdots \quad \psi_n - \psi_{ref} \quad B_{zX} \quad B_{rX}\right]^T$$

is a vector representation of control errors, ψ_i is the flux at boundary point i, ψ_{ref} is the reference flux (defined for the plasma in Fig. 2 as the flux at the X-point), and B_{rX}, B_{zX} are the radial and vertical magnetic field values at the target X-point location. In this paper, fluxes are in units of Webers per radian (Wb/rad) and fields in Tesla (T). Reducing magnetic field to zero at a target location has the effect of moving the X-point to that location. The pseudo-inverse of the matrix G is computed to produce a "decoupling matrix" G^+. Decoupled control vectors are defined by setting a single element of b equal to 1 and all others equal to 0. This means that the control vectors to provide decoupled control of the boundary points are given by columns 1 through n of G^+ and the control vectors to control radial and vertical position, respectively, of the X-point are the last two columns of G^+.

C. Decoupling Plasma Current Control from Shape Control

This approach to decoupling for shape control can be extended to include simultaneous control of the plasma current I_p. In devices that have operated for many years, one or more ohmic coils are dedicated to initiating the plasma and maintaining the desired I_p value. In more modern devices such as EAST, KSTAR, and the next-generation ITER device, no such dedicated coil exists [10]. The main idea that can be exploited in decoupling I_p and boundary control is the concept of *ohmic flux*, which is a poloidal flux distribution that is constant over the plasma cross-section. A constant flux distribution implies zero magnetic field and therefore no effect on the plasma boundary shape (see [11]). A time-varying (therefore nonzero) flux is necessary for control of Ip, since the mechanism for ohmic drive of plasma current is the generated electric field proportional to the derivative of this flux (see Tutorial 9 in [5]). Ohmic flux is actually an idealization, but well-designed ohmic coils such as those in DIII-D can approach this ideal with a good approximation. For devices with no dedicated ohmic coil, I_p control must be integrated with shape control, but the concept of ohmic flux is still useful.

An a*pproximate ohmic vector* of PF currents can be constructed that minimizes its effect on shape control parameters, in this case the flux at control points and the field at the X-points. Flux must be nonzero in order to produce ohmic current drive. To decouple the Ip drive from the shape control, the ohmic current vector should ideally produce the same nonzero flux value at all control points and at the X-points, so that perturbations to control point errors (defined as differences between flux at control points and at the X point) induced by the ohmic vector are zero. It is seldom possible to obtain the same flux identically at all points, so increasing the total flux, which is needed to ohmically drive I_p, also increases the error disturbance.

Plasma current control can be integrated with shape control by extending the matrix G and vector b in Section III.B with one additional row, representing the reference flux ψ_{ref}. For a plasma with a single X point, known as a single null plasma (Fig. 2), the vector b becomes

$$b = \left[\psi_1 - \psi_{ref} \quad \psi_2 - \psi_{ref} \quad \cdots \quad \psi_n - \psi_{ref} \quad \psi_{ref} \quad B_{zX} \quad B_{rX}\right]^T$$

Constructing the pseudo-inverse, the additional decoupling vector for I_p control is given by column n+1 of G^+.

The decoupling calculation can also be extended to plasmas having two X-points (known as double-null), such as the KSTAR plasma shown in Figure 3, which shows a cross-section of the KSTAR tokamak with the plasma boundary in red. The target boundary control point locations are shown as green circles and the two X-point targets as green crosses. In this case, the vector b is defined by

$$b = \left[\psi_1 - \psi_{ref} \quad \cdots \quad \psi_n - \psi_{ref} \quad \psi_{ref} \quad B_{zX1} \quad B_{zX2} \quad B_{rX1} \quad B_{rX2} \quad \psi_{X1} - \psi_{X2}\right]^T \tag{5}$$

where the flux at either the top or bottom X-point can be chosen as the reference flux ψ_{ref}.

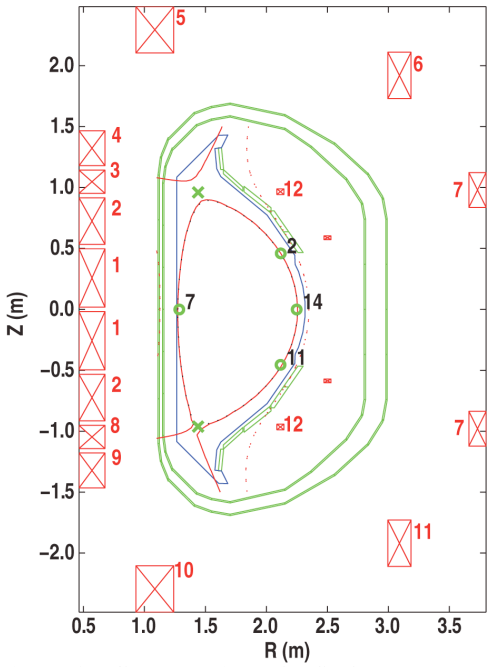

Figure 3. Cross-section of KSTAR tokamak with plasma from shot 5516. Independently controlled coil circuits are numbered in red (some coils are connected in series). Boundary control point targets used during the last plasma campaign are numbered in black. X-point target locations are indicated by green crosses.

As an example of the decoupling calculation, the matrix G in (4), with b given by (5), was computed from two different models, one including plasma motion effects, i.e. including the terms involving r_C and z_C in (3), and the other not including plasma effects. The pseudo-inverse G^+ of G was calculated for each. Depending on the condition of the matrix G, the pseudo-inverse calculation can produce columns of G^+ having very large magnitudes. In practical terms, this would mean very large changes in current in PF coils would be requested by the decoupling controller. To mitigate this problem, we actually consider $\tilde{G}I_c = \tilde{b}$, where

$$\tilde{G} = W\begin{bmatrix} G \\ \mathbf{I} \end{bmatrix}, \quad \tilde{b} = \left[b^T \quad I_c^T\right]^T,$$

$\mathbf{I}$ is the identity matrix, and W is a weighting matrix with diagonal elements equal to 1000 for rows corresponding to flux and field errors and equal to 1×10^{-3} for rows corresponding to coil currents.

This weighting is effectively a method of defining "equivalent" magnitude errors and implies in this case that flux errors on the order of 1 milliWeber per radian (mWb/rad), field errors on the order of 1 milliTesla (mT), and coil current "errors" of 1 kiloAmp are equivalent.

Figures 4 through 7 show examples of the decoupling that can be achieved with the choice of control points in Figure 3, with calculations performed using a plasma model shown in blue and vacuum model calculations in red. The top frame in each Figure is a plot of the column of G^+ corresponding to the control error defined in the caption. The bottom frame is the calculated response of control errors to the current distribution shown in top frame. Plots are shown in units of mWb/rad and mT because these are the order of magnitude changes comparable to desired control accuracy. Control points on the plasma boundary (only 4 of which are used in this example) are numbered 1 through 18, followed by the reference flux ψ_{ref}, vertical fields B_{zX1} and B_{zX2} at the X-points, radial fields B_{rX1} and B_{rX2} at the X-points, and the difference $\psi_{X1} - \psi_{X2}$ between flux values at the X-points. The requested value for this difference is set to zero if it is desired for the flux contour representing the plasma boundary to pass through both X-points.

In Figures 4 and 5, calculations for the boundary control point errors 2 and 7 are shown. Note that control point 7 error control shows very good decoupling, since there are several independently controlled coils in proximity to that point. In contrast, the error at control point 2 remains fairly strongly coupled to control point 14, for example, since the number of independently controlled coils (circuits 6 and 7) in proximity to these control points is low, and the points are rather closely spaced relative to this proximity. There is a similar difficulty in decoupling the errors at control points 11 and 14.

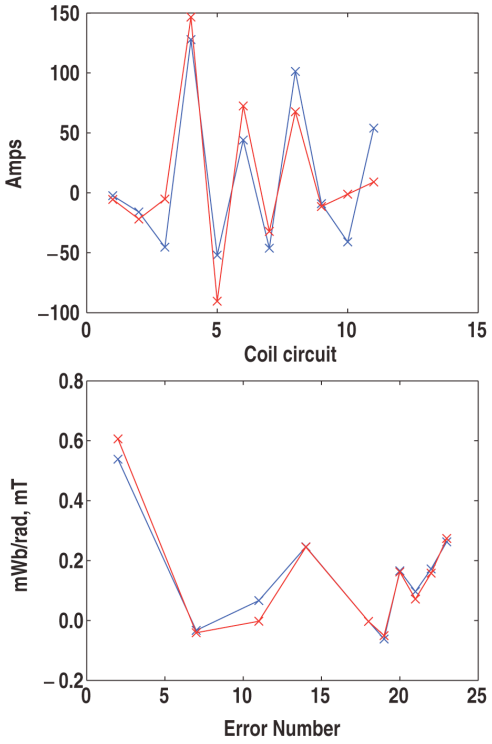

Figure 4. Calculation of decoupling vector for control point 2. The top frame in this figure and the next shows the amplitude in each coil circuit needed to obtain the best achievable approximation to 1mWb per radian change in error signal at the specified control location and zero change for other errors.

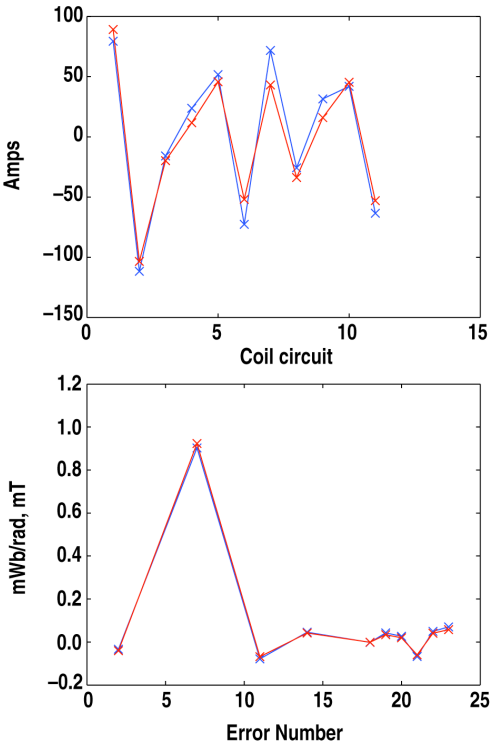

Figure 5. Calculation of decoupling vector for control point 7.

Although the control vectors computed from the vacuum model appear similar to those computed from the plasma model and both seem to provide similar decoupling, they are sufficiently different that reliance on the vacuum response can create potential problems with control. Figures 8 and 9 show examples of the result of multiplying the response matrix G that includes the plasma response by the control vectors G^{+} computed using only vacuum response. Both Figures show that there is a substantial degradation of decoupling. Using the vacuum decoupling vector to control the control point 2 error would in fact cause the error to increase rather than decrease.

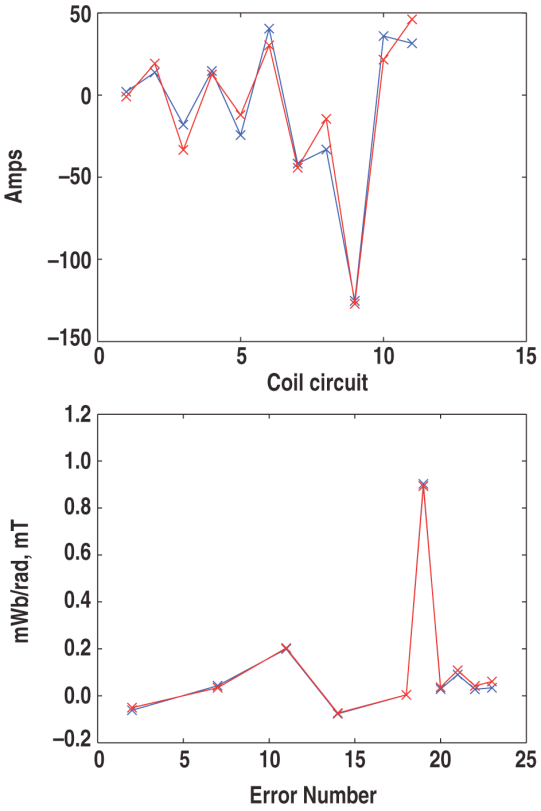

Figure 6. Calculation of decoupling vector for $\tilde{B_z}$ at X point 1. The top frame shows the amplitude in each coil circuit needed to obtain the best achievable approximation to 1mT change in magnetic field at the specified control location while not changing any other error.

In some devices, practical issues constrain the use of certain combinations of coil currents. For example, under some conditions in certain devices, coil currents cannot cross zero. In other cases, operator preferences impose such constraints. In Figure 7 we see that some of the currents in the approximate ohmic flux vector are negative, which can be undesirable. We may wish to impose a constraint that all currents in the ohmic flux decoupling vector be non-negative or even that elements corresponding to the outer coil circuits (6, 7, and 11) should be zero. In general, we can impose inequality or equality constraints on decoupling vectors by noting that the pseudo-inverse is simply a convenient

method of solving the minimization problem

$$\min\left(\left\|GI_c - b\right\|^2\right)$$

for coil currents I_c, for each of multiple vectors b. That is, for each of the vectors b with a single non-zero element described above, the least-squares solution is given by $I_c = G^{+}b$. To constrain the choice of combinations of current, we may solve the constrained minimization problem

$$\min\left(\left\|GI_c - b\right\|^2\right), \textit{subject to } I_c(i) \geq c, I_c(j) = d$$

where i and j are (mutually exclusive) sets of indices and c and d are real vectors of length equal to the number of elements in i and j, respectively.

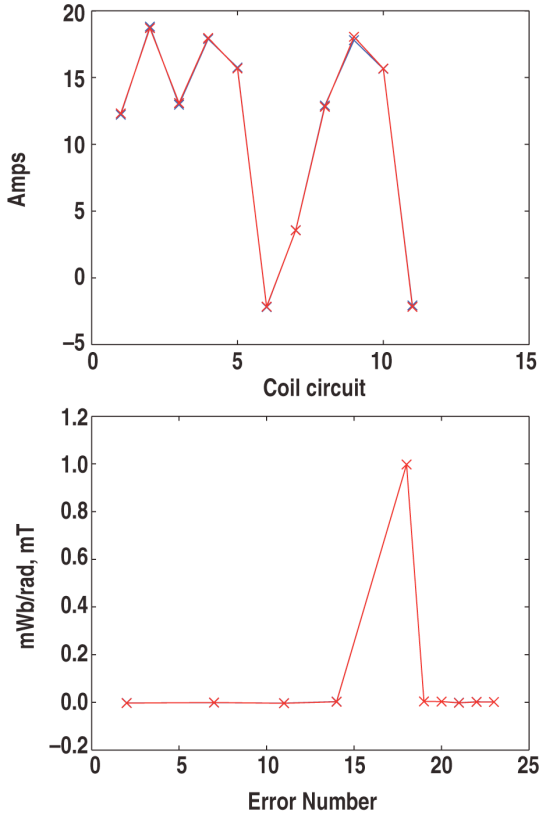

Figure 7. Calculation of decoupling vector for reference flux. Note that the inner PF coils (coil circuits 1 through 5 and 8 through 10) naturally carry most of current.

Although in general we should expect a reduction in the decoupling capability, in the case that coil currents are constrained to be nonnegative the degradation is minor, as seen in Figure 10.

D. Decoupling Vertical Control from Shape and Plasma Current Control

The discussions in sections B and C implicitly assume that the plant being controlled is open-loop stable. For high-performance plasmas the plant is in fact open-loop unstable. For an equilibrium whose plasma boundary is sufficiently vertically elongated (i.e., tall and thin), the system (1) possesses a single positive real eigenvalue. The eigenvector corresponding to the unstable root corresponds to a nearly rigid vertical motion of the spatially-distributed plasma current, hence the name *vertical instability*.

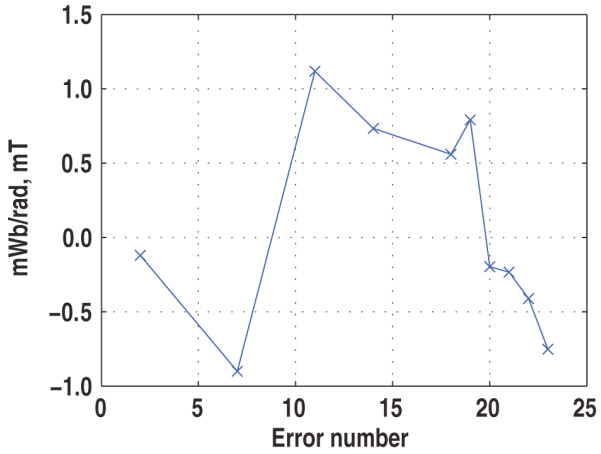

Figure 8. Product of G and control point 2 decoupling vector calculated from vacuum model.

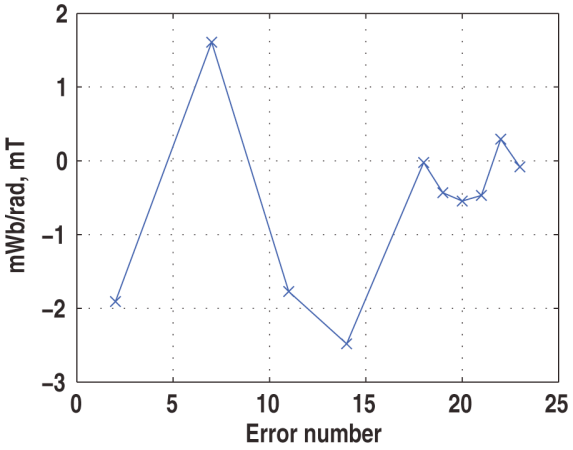

Figure 9. Product of G and control point 7 decoupling vector calculated from vacuum model.

To support high elongation, vertical stabilization typically must operate on a faster time scale than what is necessary for shape control. For this reason, the vertical control is most often implemented as a separate control loop, which enables lower cost control coils and power supplies for the slower shape and I_p control. In previous sections we have assumed the vertical control to be in place to produce the stable plant for shape and I_p control design. Although it is possible in principle to construct a single controller that simultaneously stabilizes the plasma and controls the plasma boundary, we are not aware of any existing high performance device that routinely uses such an integrated controller.

Stabilization of the instability requires a feedback control loop that produces radial magnetic field across the plasma in response to changes in some measure of the plasma vertical position, typically the plasma current centroid position

z_C [3]. The vertical control portion of a tokamak shape and stability feedback system often takes the (PD) form

$$\delta V = -K_p (z_C - z_{C,ref}) - K_d \, dz_C / dt \quad , \qquad (6)$$

where δV is the voltage applied to the PF coils in addition to that needed to maintain the operating point, $z_C - z_{C,ref}$ is the displacement of z_C from some reference position $z_{C,ref}$, and dz_C / dt is the vertical velocity of the plasma. The gains K_p and K_d are vectors which map the scalar errors to the set of PF coils involved in the vertical control.

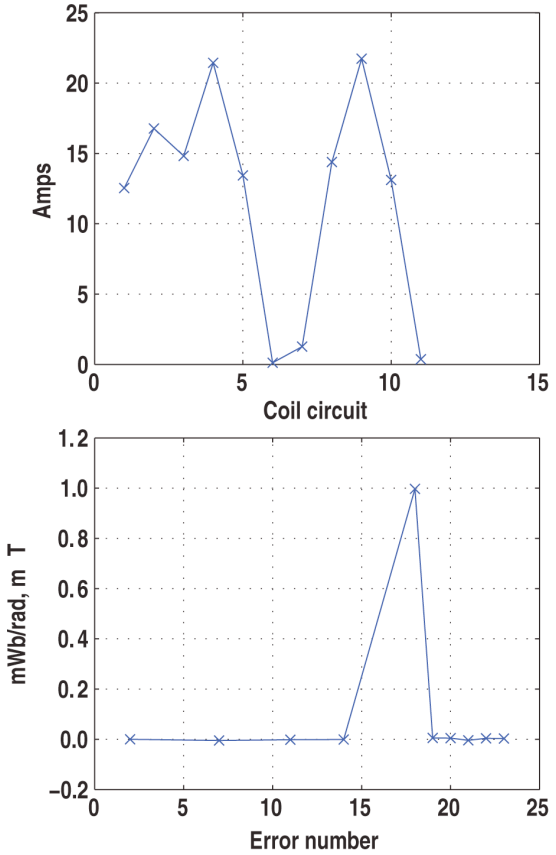

Figure 10. Calculation of decoupling vector for reference flux with the added constraint that all currents in the decoupling vector should be nonnegative.

The standard approach to decoupling the vertical control and shape/Ip control loops is to separate them in the frequency domain. The shape and I_P control operates at low frequencies, while a significant portion of the vertical stabilization control operates at high frequencies. Although primarily operating in different control bands, there are interactions between the vertical control loop and the shape and I_p control loop. The relatively slow disturbance to the vertical control due to variations of shape/I_p control coil currents are typically easily handled by the faster control. Variations in vertical control currents are usually considered to be fast disturbances on the shape and I_p control, but these disturbances can actually extend down to dc if the vertical control feedback possesses a proportional gain. In some cases, the proportional gain can be replaced by feedback on currents in the coils used for the stabilization loop [12], which attempts to keep the stabilization coil currents near zero and therefore minimize disturbances on the shape/Ip control. The JET tokamak uses a version of this approach [13]. However, there is no theory that defines generally when this substitution will (or will not) work. Another approach is to use the shape control outer loop to provide the necessary proportional gain. This approach is sometimes used in control of the DIII-D tokamak.

A primary cause of the conflict between vertical and shape control can be viewed as the difference in target position of the plasma in the two loops. The target for vertical control is typically a user-specified, often constant, value while the shape control implied target for vertical position is the centroid vertical position that is physically consistent with the user-specified boundary location. This latter value can change during the discharge depending on controlled changes to the boundary and uncontrolled variation in the spatial distribution of current within the plasma.

Another alternative to address this conflict is to use a target centroid position for the vertical control loop that is consistent with the target boundary for the shape control. Although theoretically this target centroid position could be computed off-line prior to the discharge, it requires advance knowledge of how the plasma current will be distributed spatially which, in current devices at least, is not possible. An on-line method that is used in EAST computes a vertical offset between the actual plasma current centroid derived from a real time equilibrium reconstruction algorithm and the target Z position used for the vertical control loop. Based on this calculation, the vertical control target Z value is adjusted to more closely match the actual centroid position. Conflicts that occurred between the vertical control and shape control during initial deployment of the real time reconstruction and isoflux shape control algorithms on EAST were largely eliminated using this method.

IV. LIMITATIONS OF STATIC DECOUPLING

Although the static decoupling approach is intuitively appealing, it has some limitations that must be understood in evaluating its potential extension from present devices to control of ITER. The work that is summarized in [9] highlighted two key limitations of static decoupling while finding ways to address them. First, as seen above it is not always easy to choose boundary control locations that are easily decoupled yet allow control of important boundary characteristics. This difficulty is manifested as a poorly conditioned mapping matrix G. To address this problem, the method in [9] starts with a relatively large number (32) of

boundary control points, then reduces the number of controlled parameters to scalar multipliers of singular vectors associated with largest (approximately 5) singular values of G. In ITER the boundary control locations are fixed, but small in number (6) relative to the number of independent control coil circuits (11) and are also fairly widely spaced, both of which help keep the matrix G well-conditioned.

The second issue is the need for control coil currents to remain proportional to the controller-specified sum of decoupling vectors, to avoid undesirable transient behavior of the boundary. For example, it is important to avoid transient contact of the plasma with the wall for more than a short time when the plasma has sufficiently high energy content. This requirement to maintain the controller-specified *directionality* of control currents in response to errors motivates use of actuators with similar response times. The solution used in [9] and applied to JET plasmas is to artificially slow down all coils to match the slowest response. This approach seems to sacrifice some control performance, since speed of actuator response is correlated with disturbance rejection capability. In fact, use of coil currents as actuators implies the existence of a feedback loop that commands power supply voltages to generate requested coil currents. This additional feedback loop may produce additional slowing relative to the intrinsic response capability of the open-loop commanded power supplies and coils. However, the resulting performance of an artificially slowed set of control coils may be adequate for ITER, where the time response of boundary control parameters is slow.

ACKNOWLEDGMENT

We gratefully acknowledge the collaboration of our colleagues in the EAST and KSTAR programs, especially Prof. Bingjia Xiao and Dr. Sang-hee Hahn. The needs of these programs provided the motivation for the present work.

REFERENCES

[1] Aymar, R., et. al., Overview of ITER-FEAT – The Future International Burning Plasma Experiment, Nucl. Fusion 41 (2001) 1301.

[2] M. L. Walker, D. A. Humphreys: On feedback stabilization of the tokamak plasma vertical instability. Automatica 45(3): 665-674 (2009)

[3] A. Pironti and M.L.Walker, Fusion, Tokamaks, and Plasma Control: An introduction and tutorial, *IEEE Control Systems Magazine*, vol. **25**, no. 5, pp. 31–43, 2005

[4] M.L.Walker and D.A.Humphreys, Valid coordinate systems for linearized plasma shape response models in tokamaks, Fusion Science and Technology, v. 50, Nov. 2006, p. 473-489

[5] A. Beghi and A. Cenedese, Advances in Real-Time Plasma Boundary Reconstruction, *IEEE Control Systems Magazine*, vol. **25**, no. 5, 2005, 44-64

[6] J. Wesson, Tokamaks, 3rd Ed., Oxford University Press, 2004

[7] Q-G Wang, Decoupling Control, Lecture Notes in Control and Information Sciences 285, Springer, 2003

[8] F.Hofmann, S.C. Jardin, Plasma Shape and Position Control in Highly Elongated Tokamaks, Nuc. Fus. 30, no. 10, 1990, 2013-2022

[9] M. Ariola and A. Pironti, Plasma Shape Control for the JET Tokamak: An optimal output regulation approach, *IEEE Control Systems Magazine*, vol. **25**, no. 5, pp. 65–75, 2005

[10] J. A. Leuer, Plasma Startup Design of Fully Superconducting Tokamaks EAST and KSTAR With Implications for ITER, IEEE Trans. Plasma Sci., v.. 38, no. 3, March 2010, 333

[11] G. Ambrosino and R. Albanese, Magnetic Control of Plasma Current, Position, and Shape in Tokamaks, A survey of modeling and control approaches, *IEEE Control Systems Magazine*, vol. **25**, no. 5, 2005, 76-92

[12] G. Ambrosino, et.al., Plasma position and shape control in ITER using in-vessel coils, Proceedings of the 47th IEEE Conference on Decision and Control Cancun, Mexico, Dec. 9-11, 2008, 3139

[13] F. Sartori, G. deTommasi, F. Piccolo, The Joint European Torus, Plasma position and shape control in the world's largest tokamak, *IEEE Control Systems Magazine*, vol. **26**, no. 2, pp. 64–78, 2006